OVLBI-ES Memo 81

GBES Antenna Pointing Offsets for 2001

Glen Langston

2001 October 30

Overview

This document describes the measurement of OVLBI GBES antenna pointing corrections in 2001 October. The pointing coefficients are measured by observing astronomical radio sources and fitting the differences between observed and predicted positions. The pointing offset function is described and previous measurements of the coefficients listed. After calculating and applying a pointing correction model, the 1 sigma residual pointing errors are 0.9 arc-minutes in azimuth and 1.1 arc-minutes in elevation.

These observations were made to search for sudden changes in the pointing model. No clear evidence for such changes was found, although there is greater range in the pointing offsets at low elevation.

Introduction

Bright compact radio sources were observed with the GBES antenna on 2001 October 26 and 27. The offsets between the known source location (in azimuth, elevation) and encoder readings of at location of signal maximum were recorded.

The antenna pointing error model described in GBES Memo 31 (Murphy and D'Addario) was used to measure the antenna pointing offsets. Previous observations are described in GBES Memo 57, entitled "GBES Antenna Pointing Offsets for 1994" by G. Langston.

The pointing model consists of two equations, one for Elevation offset and one for Azimuth Offset, given below:

$$\Delta el = C_1 + C_2 \cos(az) + C_3 \sin(az) + C_4 \cos(el)$$

and

$$\Delta az \ \cos(el) = C_5 \cos(el) + C_6 \cos(az) \sin(el) + C_7 \sin(az) \sin(el) + C_8 \sin(el) + C_9$$

The coefficients are interpreted as follows:

C_1, C_5 Elevation encoder and collimation.

C_2, C_7 Elevation axis error.

C_3, C_6 Azimuth axis error.

C_4 Gravitational sag of the antenna.

Table 1: Measurements of the GBES pointing coefficients. The 1994 April 12 to 21 measurements are without the FFS and ellipsoidal mirror. All measurements after 94 April 25 are made with the FFS and ellipsoidal mirror. After 1994 April 21, the relationships between the coefficients were enforced: $C[2] \equiv C[7]$ and $C[3] \equiv -C[6]$.

	940412	940415	940421	940429	940807	000630	011026
C[1]	8.66±0.25	-1.52	2.62±0.31	-5.87±0.27	-7.08±0.25	-22.78	-22.20±0.11
C[2]	4.73±0.14	-5.20	4.69±0.12	5.28±0.10	4.98±0.13	5.02	4.65±0.02
C[3]	-6.00±0.10	-5.11	-6.37±0.10	-6.61±0.12	-6.48±0.13	-5.58	-4.36±0.02
C[4]	-0.08±0.36	-2.17	-1.88±0.41	-1.82±0.33	-1.22±0.34	-0.60	-1.56±0.14
C[5]	18.74±1.32	14.16	8.95±1.08	14.20±1.05	13.95±0.99	15.96	14.74±0.44
C[6]	5.99±0.19	5.11	6.20±0.17	6.61±0.12	6.48±0.13	5.58	4.36±0.02
C[7]	6.39±0.15	5.20	4.52±0.16	5.28±0.10	4.98±0.13	5.02	4.65±0.02
C[8]	2.97±1.34	-0.53	-3.03±0.90	-1.05±0.83	-1.82±0.96	-2.79	-2.78±0.38
C[9]	-7.13±1.77	0.81	4.98±1.32	-4.11±1.26	-2.89±1.27	-3.36	-2.10±0.54

C_8 Represents the non-perpendicularity of the axes.

C_9 Represents the non-perpendicularity of the beam and elevation axis.

In memo 31, the fitted pointing coefficients are listed. In table 1, the last few measurements are recorded, along with the latest measurements, using a new method. The newest measurements were taken under rather poor observing conditions. Also the 94 April 7-12, measurements are *not* corrected for refraction. However these measurements were taken at elevation > 30 degrees and refraction is a small addition to the pointing offsets.

The measurements after 94 April 15 are corrected for refraction effects, and include a first order correction for the sky effects on the baseline data. Between April 15 and April 21, a number of adjustments to the focus, rotation and tilt of the sub-reflector were make. These adjustments were known to effect these pointing coefficients.

On 94 April 25, the subreflector was rotated 180 degrees and the ellipsoidal mirror installed. The optical path to the Ku band feed, then included a reflection off the Frequency Selective Surface (FSS) to the ellipsoidal mirror and then to the Ku Band feed. The subreflector rotation was set to 4.95 volts, and the subreflector focus was set to 1.24 volts.

On 94 August 7, the antenna pointing was again measured. During these measurements, both the X and Ku band Front End electronics were installed. The pointing coefficients were calculated based on measurements with the X-band feed LCP polarization. Figures 1 - 9 show the measured data and a comparison of measurements and the model fit for the 94 August 7 observations. The discrepancies in the model and fit are mostly due to errors in a few points from the fainter radio sources.

Between 1994 and 2001, the elevation encoder was replaced once and adjusted again in June 2000. At this time the zero point offset in the encoder was shifted. This explains the jump in coefficient C[1] between the two epochs.

The observations made on 2001 Oct 26 and 27 appeared to have much greater RMS near

azimuth = 0, where the CASA observations are made at low elevation. All low elevation CASA data were removed before fitting. The azimuth and elevation coefficients in 2001 were fit simultaneously enforcing the fixed relationship between some azimuth and elevation coefficients. The was only a small difference between coefficient values for dependent and independent fits.

Conclusions

The method for calculating the GBES pointing coefficients produces a fit with small residual errors. The RMS of the residuals after compensating for pointing errors is 0.88 arc-minute in azimuth, but the variation in Elevation values is greater, 1.1 arc-minutes.

Generally the azimuth and elevation residuals are Gaussian distributed with zero mean, after the pointing model corrections are applied. There does not appear to be a great variation in elevation offsets. There does appear to be a small systematic variation in azimuth residual as a function of azimuth angle. This error is not great enough to adversely effect satellite tracking.

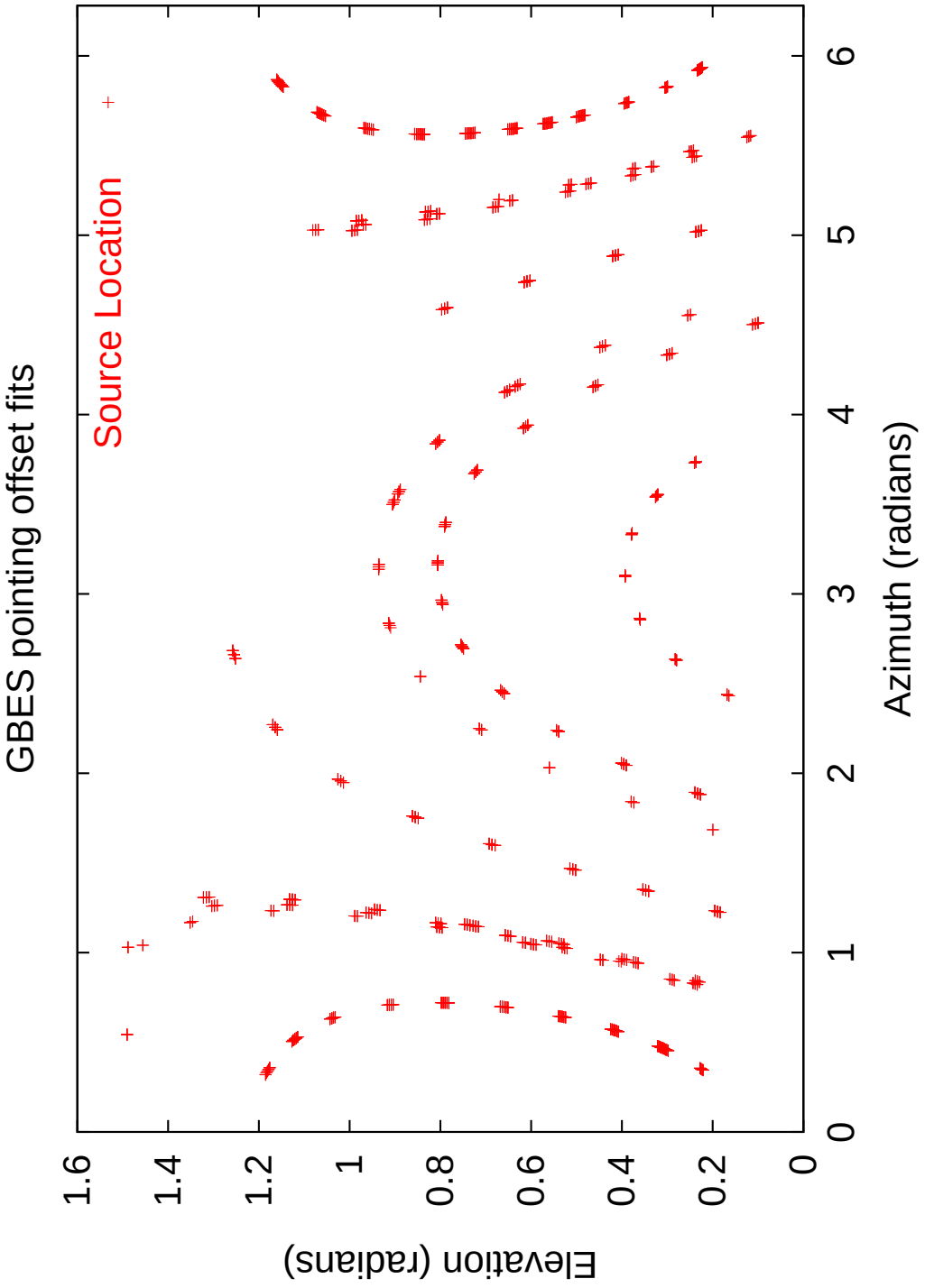

Figure 1: Plot of the Azimuth and Elevation (radians) locations of the radio sources when pointing offset measurements were taken on 1994 August 7.

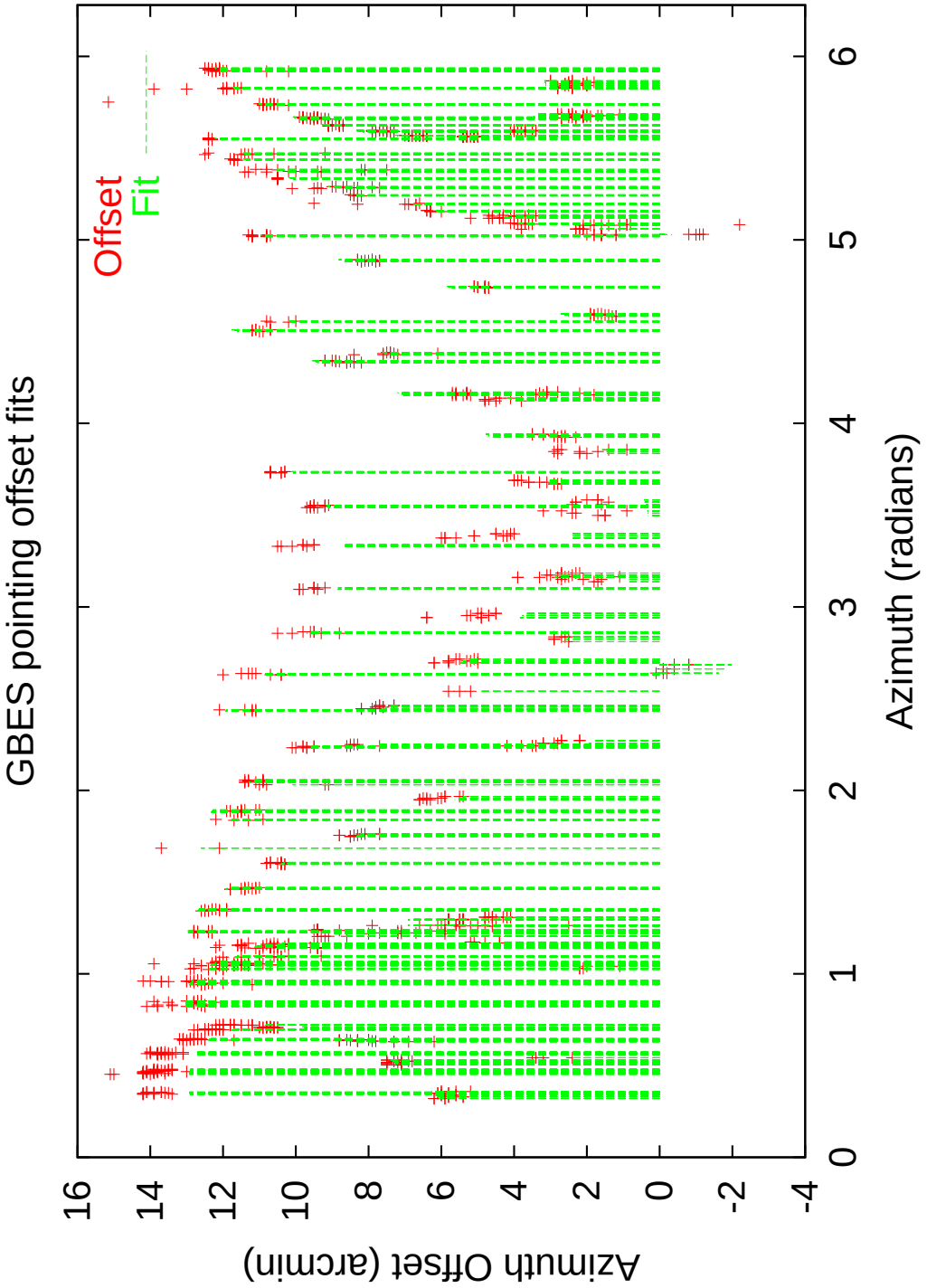

Figure 2: Plot of the Azimuth offsets (arc minutes) as a function of Azimuth (radians) of the radio sources. The measured points are marked by diamonds (⋄), and the model values are shown by dashed lines.

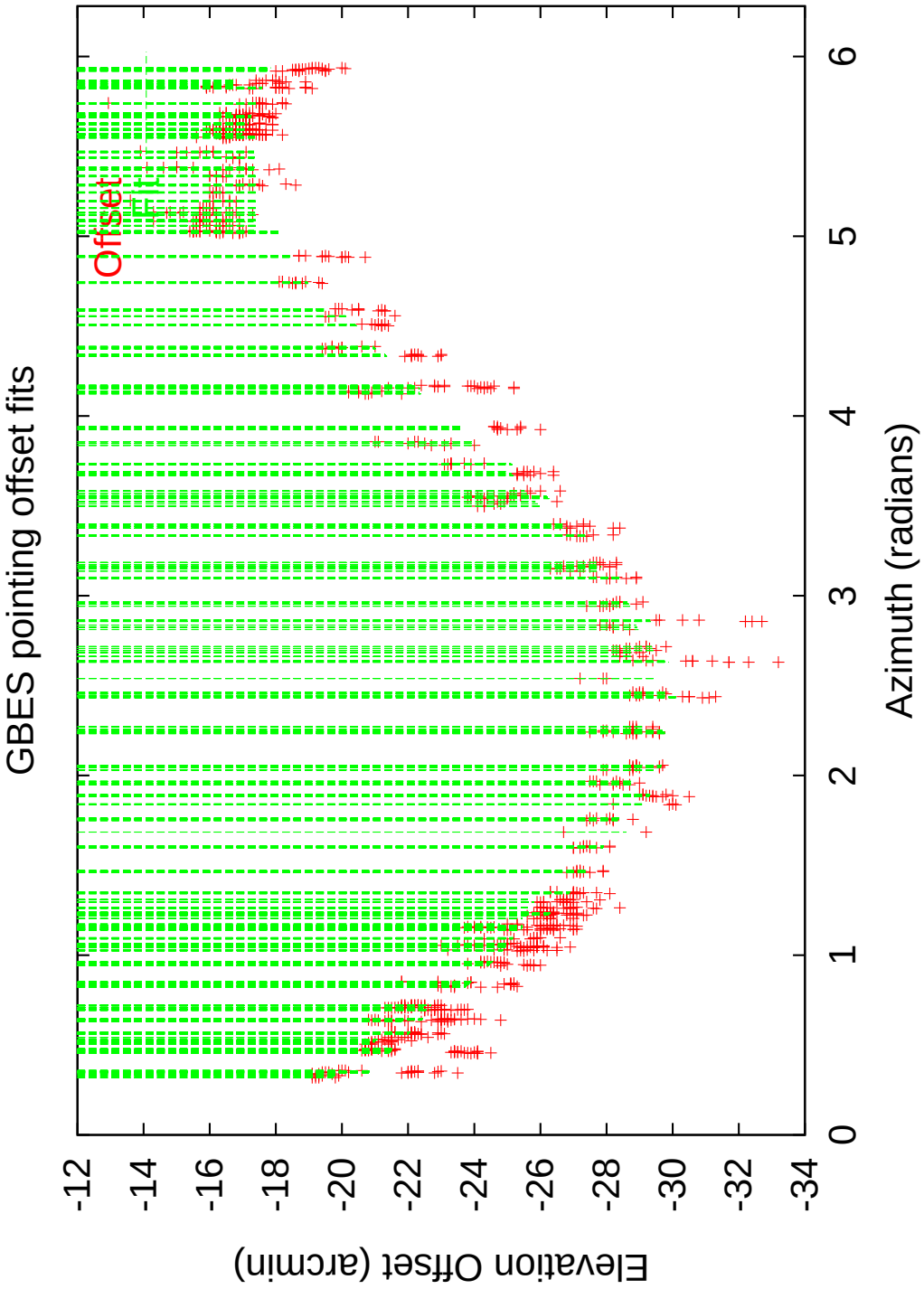

Figure 3: Plot of the Elevation offsets (arc minutes) as a function of Azimuth (radians) of the radio sources.

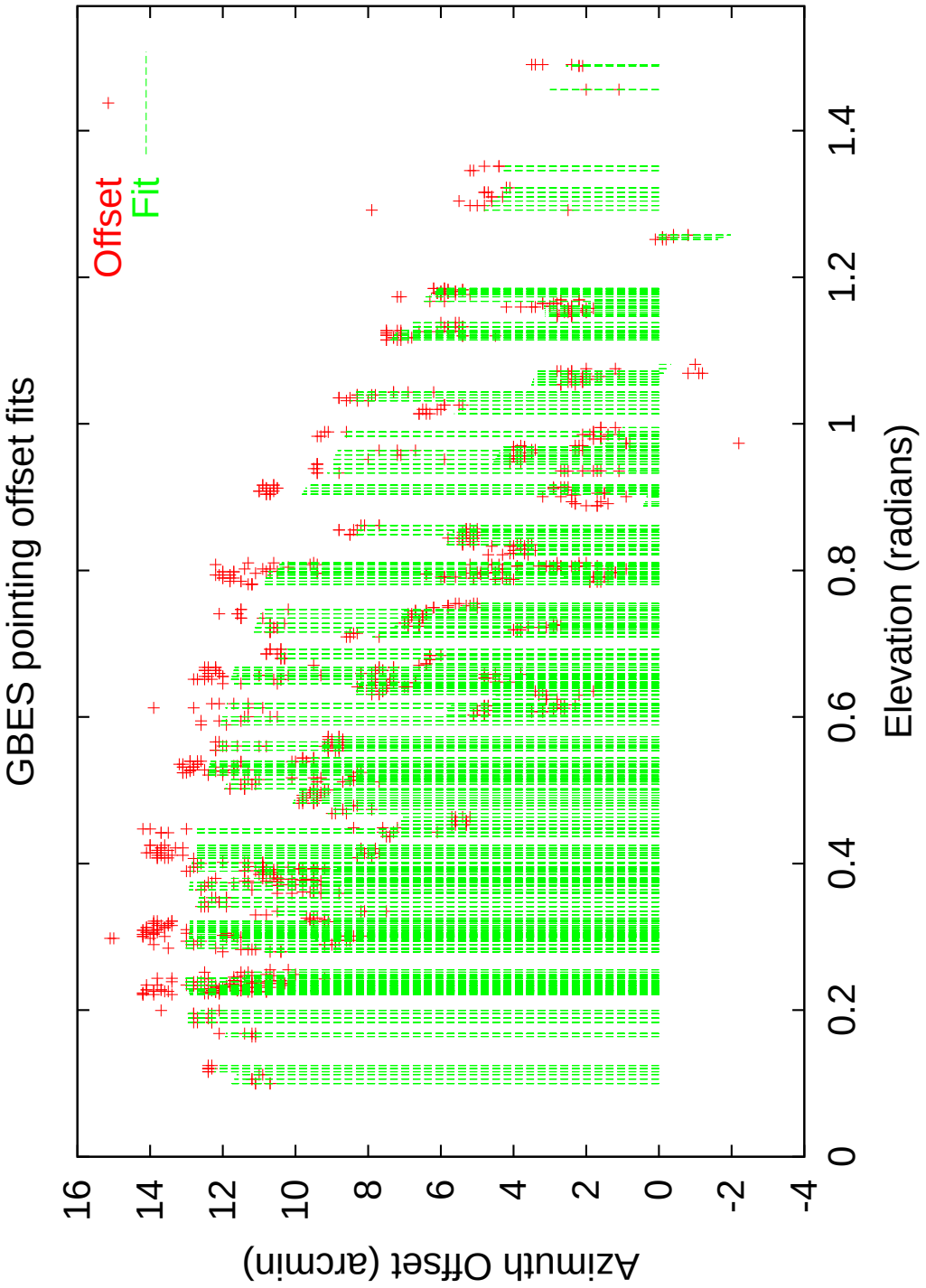

Figure 4: Plot of the Azimuth offsets (arc minutes) as a function of Elevation (radians) of the radio sources.

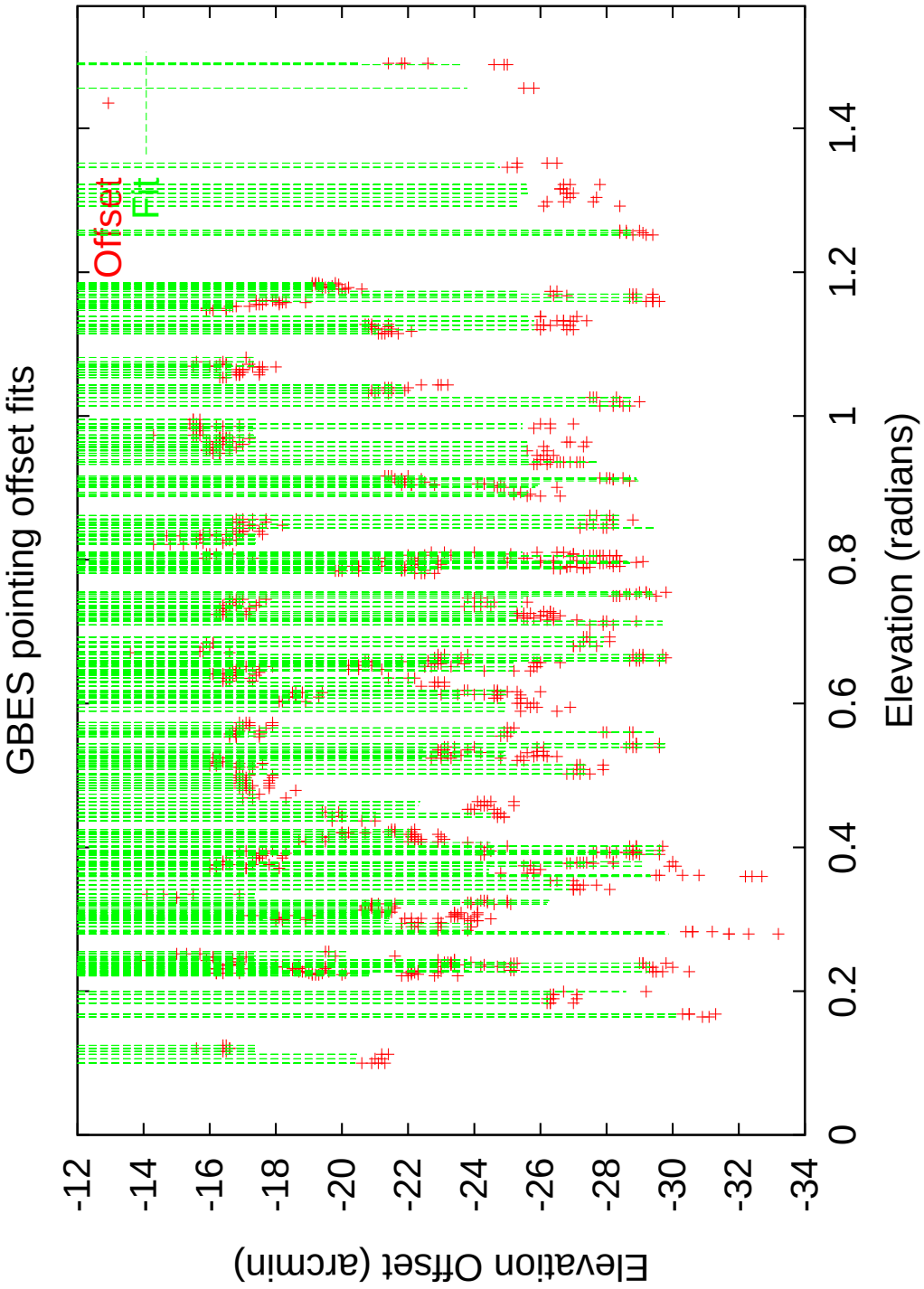

Figure 5: Plot of the Elevation offsets (arc minutes) as a function of Elevation (radians) of the radio sources.

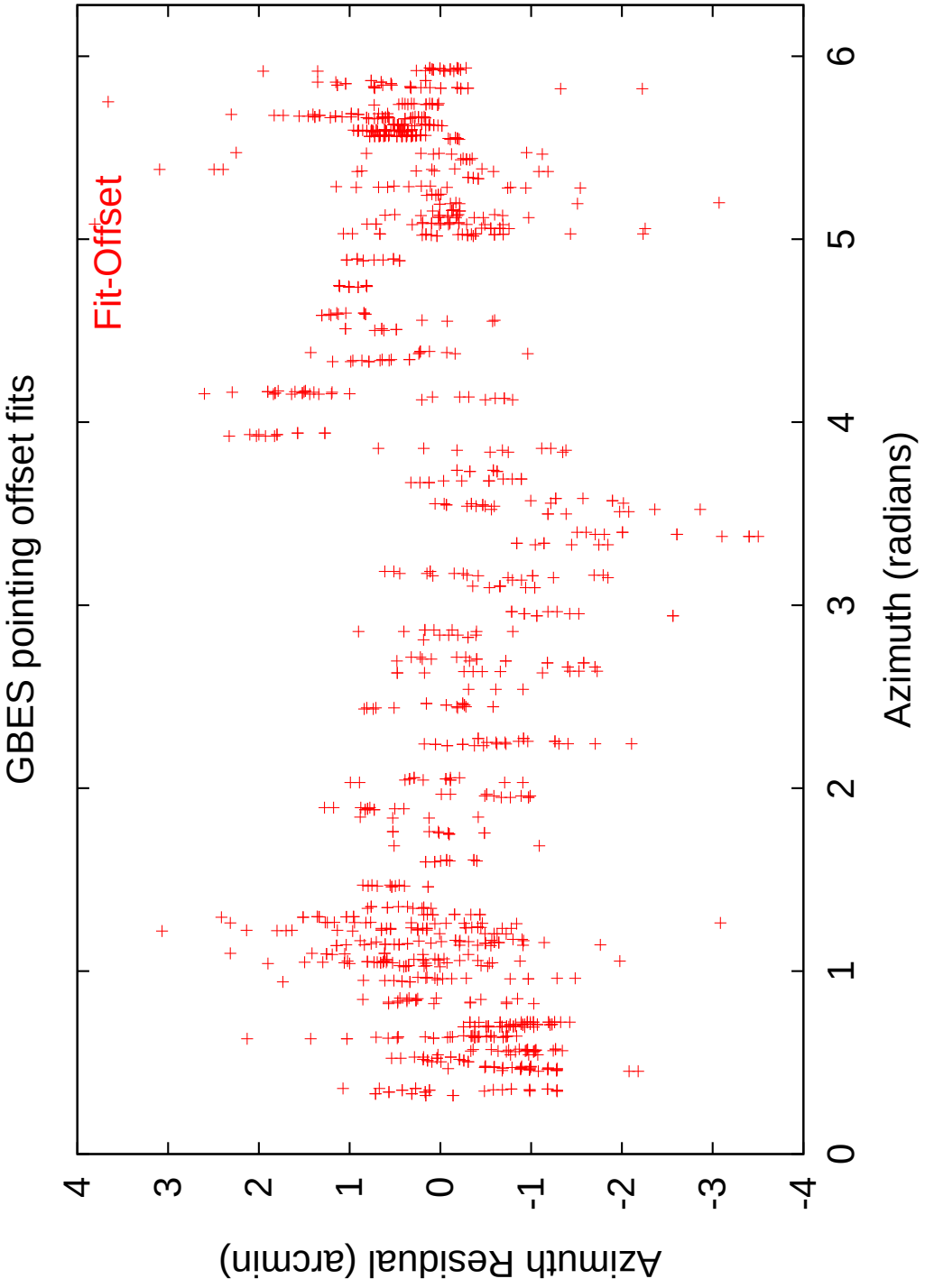

Figure 6: Plot of the Residual of the Azimuth Fit - Measured Azimuth Offsets (arc minutes) as a function of Azimuth (radians) of the radio sources.

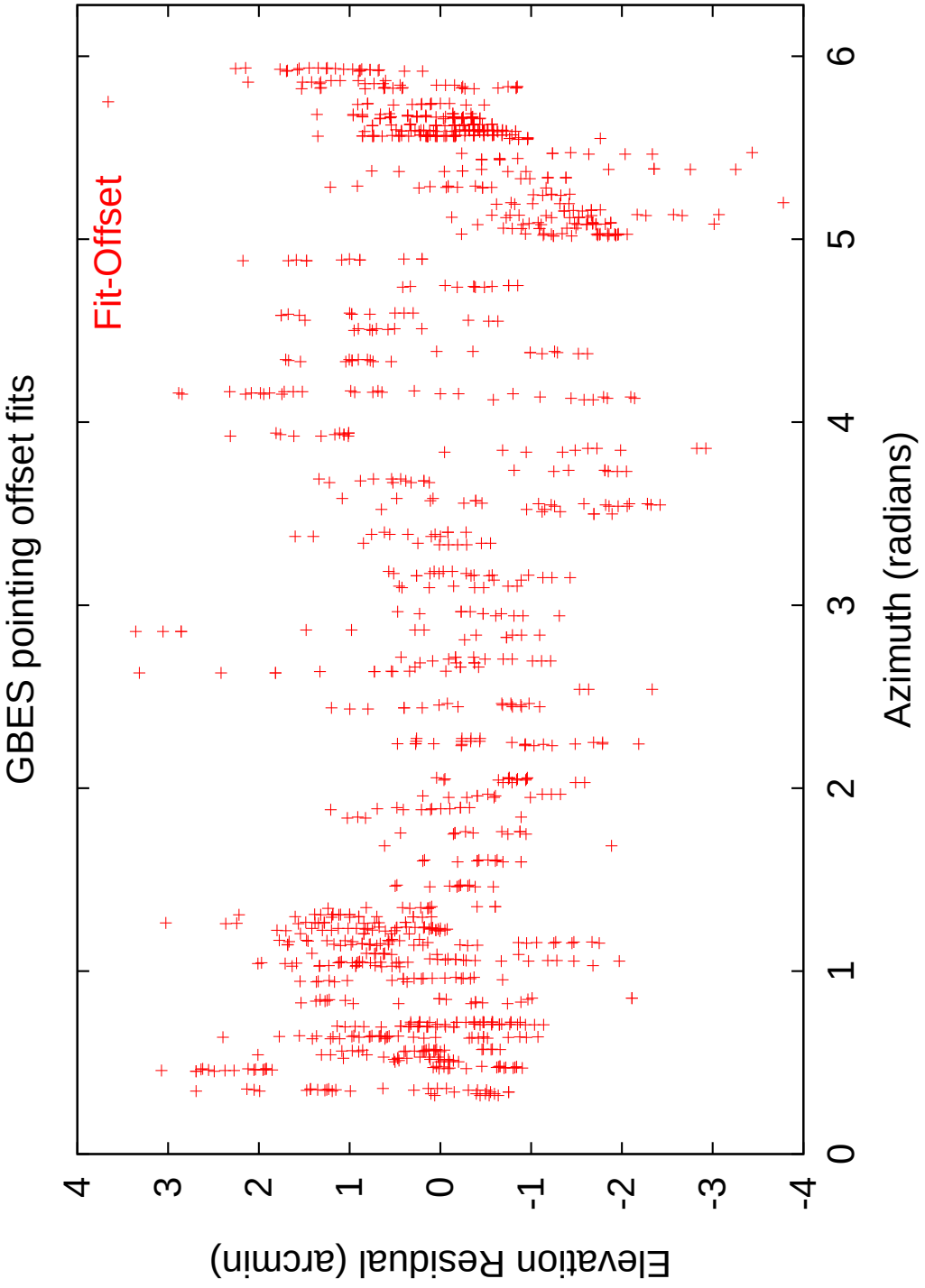

Figure 7: Plot of the Residual of the Elevation Fit - Measured Elevation Offsets (arc minutes) as a function of Azimuth (radians) of the radio sources.

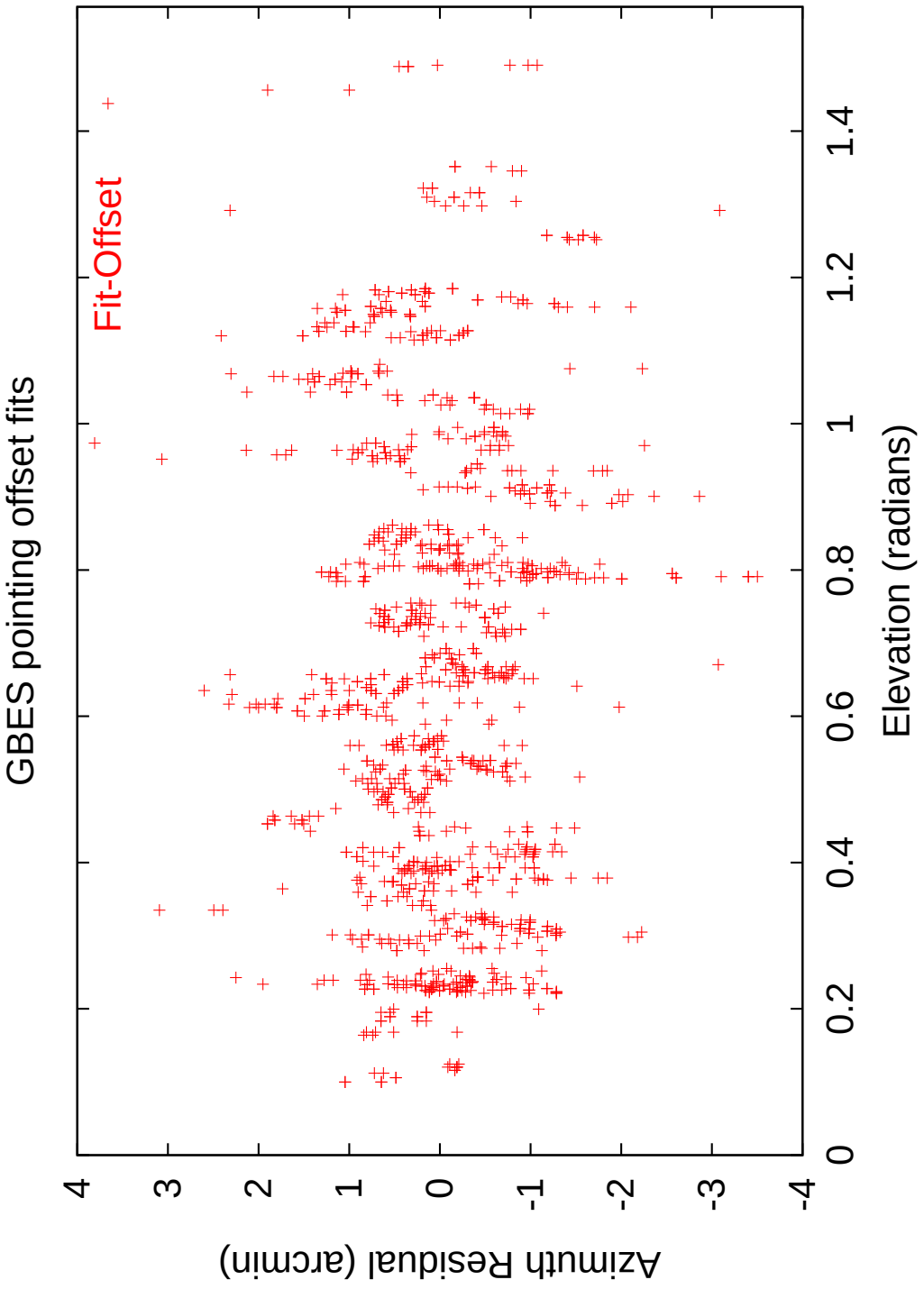

Figure 8: Plot of the Residual of the Azimuth Fit - Measured Azimuth Offsets (arc minutes) as a function of Elevation (radians) of the radio sources.

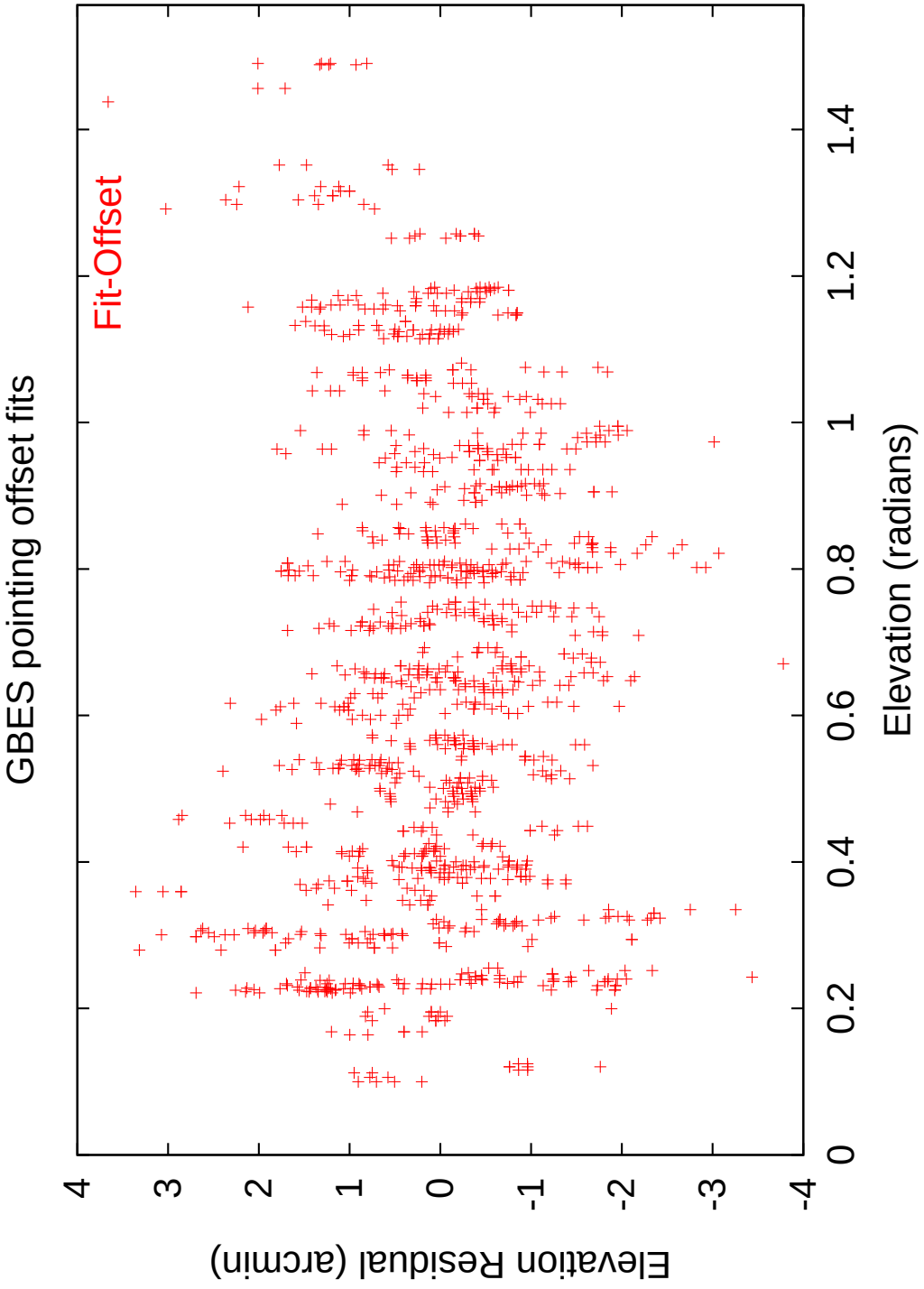

Figure 9: Plot of the Residual of the Elevation Fit - Measured Elevation Offsets (arc minutes) as a function of Elevation (radians) of the radio sources.